



Hoste, J.-J., Fossati, M., Taylor, I. and Gollan, R. (2018) Turbulence Chemistry Interaction via Eddy Dissipation Model for Scramjet Analysis and Design. 7th European Conference on Computational Fluid Dynamics (ECFD 2018), Glasgow, UK, 11-15 Jun 2018.

This is the author's final accepted version.

There may be differences between this version and the published version. You are advised to consult the publisher's version if you wish to cite from it.

<http://eprints.gla.ac.uk/162942/>

Deposited on: 18 July 2018

Enlighten – Research publications by members of the University of Glasgow
<http://eprints.gla.ac.uk>

TURBULENCE CHEMISTRY INTERACTION VIA EDDY DISSIPATION MODEL FOR SCRAMJET ANALYSIS AND DESIGN

Jimmy-John O.E. Hoste^{1,3}, Marco Fossati¹, Ian J. Taylor² and Rowan J. Gollan³

¹ University of Strathclyde
Aerospace Center of Excellence
G1 1XJ, Glasgow, United Kingdom
e-mail: jimmyjohn.hoste/marco.fossati@strath.ac.uk

² University of Glasgow
School of Engineering
G12 8QQ, Glasgow, United Kingdom
e-mail: ian.taylor@glasgow.ac.uk

³ University of Queensland
Center for Hypersonics
QLD 4072, Brisbane, Australia
e-mail: r.gollan@uq.edu.au

Key words: Scramjets, RANS, Eddy Dissipation Model

Abstract. This paper considers the Eddy Dissipation Model to address the combustion process inside scramjet engines designed to operate at high flight Mach numbers. The aim is to demonstrate the most appropriate use of the model for design purposes. To this end, two hydrogen-fueled experimental scramjet configurations with different fuel injection approaches are studied numerically. In the case of parallel fuel injection, it is demonstrated that relying on estimates of ignition delay from a one-dimensional kinetics program can greatly improve the use of the EDM. In the second case, the transverse injection of hydrogen resulted in an overall good agreement of the model with experimental pressure traces except in the vicinity of the injection location. Overall, the EDM appears to be a suitable tool for scramjet combustor design incorporating a parallel or transverse fuel injection mechanism.

1 INTRODUCTION

Scramjet technology has been the subject of many studies since the late 1950s as it provides an efficient mean of flying at hypersonic speeds. Potential applications include hypersonic cruise vehicles, missiles and access-to-space systems. The Australian SPARTAN program aims at exploring the advantages of scramjets (hydrogen fueled) by designing a three-stage-to-orbit rocket-scramjet-rocket launch system with reusable first and

second stages [1, 2]. Numerical tools with different levels of fidelity are intensively used in the design of scramjets. To illustrate this, quasi-one-dimensional models have been developed which rely on simplified assumptions to describe the supersonic combustion process [3, 4]. Being computationally cheap, such low-fidelity approaches are attractive for integration as a subsystem in complete vehicle analysis as well as in Multi-disciplinary Design Optimization (MDO). Steps are being undertaken toward the improvement of the mixing and combustion models inside these approaches by use of information from Computational Fluid Dynamics (CFD) [5]. Among the CFD formulations available to address supersonic turbulent reacting, Reynolds-Averaged Navier-Stokes (RANS) still remains the principal analysis approach for hypersonic propulsion flow paths [6, 7]. Within the RANS framework, the treatment of the turbulent combustion process is a topic of open research.

As an accelerator for access-to-space, the high flight Mach regime ($\approx 7-12$) at which a scramjet will operate is characterized by a combustion process which can be considered to be mainly mixing limited [8, 9, 10]. A good trade-off between accuracy and computational efficiency to address turbulence / chemistry interaction (TCI) for mixing-limited scramjets is the Eddy Dissipation Model (EDM) introduced by Magnussen and Hjertager [11]. The EDM could therefore be relied on for the design of scramjet combustors operating at high Mach numbers whilst keeping the computational cost at a moderate level. Moreover, the EDM can potentially provide information on the mixing and combustion process to low-fidelity tools, such as quasi-one dimensional models, used in the design of vehicle integrated propulsion systems.

The use of EDM in the modeling of hydrogen-fueled scramjet flows has been reported in the literature by Edwards et al. [12] using the REACTMB in-house CFD solver as well as with commercial software by other authors [13, 14, 15, 16]. Little information is however found in the open literature about possible improvements of the model or the optimal use of the EDM for scramjets with different types of fuel injection configurations. To the best of authors' knowledge, the only work describing a possible improvement of the EDM, with potential application to scramjets, is that of Norris [17]. Norris makes use of Perfectly Stirred Reactors (PSR) and Partially-Stirred Reactors (PaSR) to tune the model before a CFD run. However, the author indicates that the method might result in poor performance in the presence of shocks and expansions. This approach is therefore not considered here.

The aim of the present work is to demonstrate the capability of the EDM in providing flow field information with a reasonable degree of accuracy such that scramjet combustor design decisions can be made in future work. More specifically, the optimal use of the model is described for two scramjet combustors representative for high equivalent flight Mach numbers. Both test cases rely on a different fuel injection scheme allowing to broaden the perspective. The paper is structured as follow. Section 2 introduces the governing equations and the combustion modeling with the EDM. Section 3 discusses the two test cases considered in the present work and conclusions are drawn in Section 4.

2 NUMERICAL MODELING

The governing equations for turbulent compressible reacting flows can be written as

Mass Conservation:

$$\frac{\partial \bar{\rho}}{\partial t} + \frac{\partial}{\partial x_i} (\bar{\rho} \tilde{u}_i) = 0 \quad (1)$$

Momentum Conservation:

$$\frac{\partial}{\partial t} (\bar{\rho} \tilde{u}_i) + \frac{\partial}{\partial x_j} (\bar{\rho} \tilde{u}_j \tilde{u}_i + \delta_{ij} \bar{p}) = \frac{\partial}{\partial x_j} \left(\bar{\tau}_{ji} - \widetilde{\bar{\rho} u_i'' u_j''} \right) \quad (2)$$

Energy Conservation:

$$\frac{\partial}{\partial t} (\bar{\rho} \tilde{E}) + \frac{\partial}{\partial x_j} (\bar{\rho} \tilde{u}_j \tilde{H}) = \frac{\partial}{\partial x_j} \left(\bar{\tau}_{ij} \tilde{u}_i + \overline{\tau_{ij} u_i''} - \bar{q}_j - \widetilde{\bar{\rho} H'' u_j''} \right) \quad (3)$$

Species Conservation:

$$\frac{\partial (\bar{\rho} \tilde{Y}_s)}{\partial t} + \frac{\partial (\bar{\rho} \tilde{Y}_s \tilde{u}_j)}{\partial x_j} = \bar{\omega}_s - \frac{\partial}{\partial x_j} \left(\bar{J}_{sj} + \widetilde{\bar{\rho} Y_s'' u_j''} \right) \quad (4)$$

with conserved variables $\bar{\rho}$, $\bar{\rho} \tilde{u}_j$, $\bar{\rho} \tilde{E}$, $\bar{\rho} \tilde{Y}_s$ representing density, momentum, total energy per unit volume and partial densities of the species s ($s=1, \dots, N$). Throughout this work, the above set of equations will be referred to as the Reynolds Averaged Navier-Stokes equations (RANS). The symbols \bar{x} and \tilde{x} denote respectively the time and Favre (or density-weighted) average. Equations (1) to (4) are written in such a way that those terms which require modeling are indicated on the right-hand side. The system of conservation equations for a turbulent chemically reacting flow needs extensive modeling. A comprehensive overview of the modeling practice for supersonic internal flows can be found in the work of Baurle [6]. The present work will only address the treatment of the mean species reaction rates $\bar{\omega}_s$.

The RANS equations are solved with the Eilmer[18, 19] open-source CFD package, developed at the University of Queensland. The finite volume solver addresses turbulence closure by means of Wilcox's 2006 $k - \omega$ model [20] and has proven to perform well for scramjet type flows [21, 22, 23]. The inviscid fluxes are treated with Liou and Wada's AUSMDV [24] scheme. An adaptive method is also available that activates the more diffusive Macrossan's Equilibrium Flux Method (EFM)[25] in regions with strong velocity gradients. Viscous fluxes are treated by means of Gauss' theorem and the time integration is performed with either the forward Euler or a predictor-corrector scheme (Heun's method). A thermally perfect gas mixture is assumed in scramjet flows where the heat capacities are temperature dependent.

2.1 Combustion Modeling

In the present work, the mean species reaction rates $\bar{\omega}_s$ is given by the Eddy Dissipation Model (EDM) introduced by Magnussen and Hjertager [11]. The EDM assumes that fuel and oxidizer, carried by separate turbulent eddies in diffusion flames, react as soon as

they mix on a molecular scale (infinitely fast chemistry). Therefore, the rate at which the reactions occur depends on a turbulent mixing time which brings eddies of fuel and oxidizer together. On dimensional basis, this mixing time is estimated from the integral length scales by using the turbulence model parameters which describe the energy cascade process in turbulent flows. Consequently, the mixing on a molecular level is dependent on the rate at which the eddies dissipate. A detailed discussion of the EDM can be found in [23] and only a restricted amount of information, relevant to this work’s considerations, is given below. In the case of hydrogen combustion, the EDM considers a global reaction ($2H_2 + O_2 \rightarrow 2H_2O$), and N_2 acting as an inert species, resulting in four species equations (Equation 4). In EDM, the reaction rate of fuel (H_2) is defined as:

$$\bar{\omega}_F = -A_{\text{edm}} \bar{\rho} \beta^* \omega \min \left[\tilde{Y}_F, \frac{\tilde{Y}_O}{s} \right] \quad (5)$$

A_{edm} is a model constants with a standard value of 4.0 which follows from the work of Magnussen and Hjertager [11] on low speed flames. The EDM can include some effects of chemical kinetics by limiting the reaction rate with a kinetic reaction rate ($\bar{\omega}_{F,\text{lam}}$). This can be done by use of the reaction rate obtained with the “no-model” or Arrhenius approach (law of mass action) and a single step global reaction [6] :

$$\bar{\omega}_F = \min(\bar{\omega}_{F,\text{edm}}, \bar{\omega}_{F,\text{lam}}) \quad (6)$$

3 Test Cases

The EDM is applied to the study of two hydrogen-fueled scramjet configurations for which experimental data is available in the open literature. The combustor entrance conditions are above Mach 2 which is representative for scramjets at high flight Mach numbers. Unit Lewis number is assumed for each species throughout this work and in case of viscous walls without wall functions, the value of ω is set according to Menter’s suggestion for smooth walls [26]. A CFL value of 0.4 is adopted for time integration.

3.1 Burrows-Kurkov

A commonly used test case in CFD code validation studies for supersonic combustion is the experiment of Burrows and Kurkov [27] (BK) shown in Figure 1 for which an extensive set of comparison data in pure mixing and reacting conditions is available. Many authors have performed RANS studies of the geometry over the last three decades including [28, 29, 30]. The test case is known to be very sensitive to the the values of turbulent Prandtl (Pr_t) and Schmidt (Sc_t) numbers. Following a sensitivity study for Wilcox $k-\omega$ 2006 model, a combinations $Pr_t = 0.5$, $Sc_t = 0.5$ is used in this work.

3.1.1 Problem Formulation

The experimental setup in Figure 1 has been simulated in two stages with the explicit Euler scheme to reach steady state and the adaptive inviscid flux treatment. More details about this procedure are given in previous work [23] which aimed at understanding the effect of the A_{edm} constant on the flow solution.

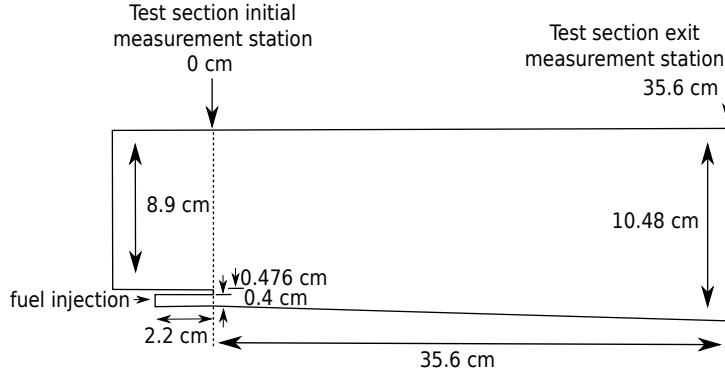


Figure 1: Schematic of the Burrows-Kurkov supersonic combustion experiment [27]. Not to scale.

3.1.2 Results

The Burrows-Kurkov combustor has been simulated with four different settings for the combustion treatment: EDM (5), EDM + kinetic limit (6), zonal EDM, finite rate chemistry (FRC) without TCI. The zonal EDM relies on an estimate of an ignition delay to create a zone in which no combustion is allowed to occur. Burrows and Kurkov [27] document an ignition delay of $90\text{e-}6$ s which was obtained using a one-dimensional kinetics program. Using an averaged vitiated air stream velocity at the entrance of the combustor of 1689 m/s (obtained from CFD), a flow length equal to $2.1\text{e-}4$ s is obtained. The latter value yields an estimate of a fluid element residence time inside the combustor. From this value and the previously calculated induction time, the ignition location inside the combustor is estimated to be at $x = 0.153$ m. No combustion is allowed at any axial location before that point. Note that this approach only gives a rough estimate of the induction process. For example, it does not account for the low fuel stream temperature near the wall which can have a significant influence as indicated by Burrows and Kurkov [27]. Nevertheless, this information can be relied on for a better use of the EDM. The FRC simulation is performed with the 7 species, 8 step reaction mechanism of Evans-Schexnayder (E-S) with modified third-body efficiencies in accordance with Bhagwandin et al. [30].

The results of the numerical simulation show that the kinetic limit only has an effect on the EDM in the vicinity of the fuel injector. Figure 2 (a) illustrates this with the contour of $Y_{\text{H}_2\text{O}}$. The observation is explained by a high vitiated air stream temperature and the use of a single-step reversible reaction with the law of mass action as a kinetic limit. Moreover, the localized effect does not affect the behavior in the downstream region of the combustor. Note that the EDM without a kinetic limit results in an unphysical behavior as fuel and oxidizer burn as soon as they mix. Experimentally [27] an ignition delay is observed between 18 (wall pressure trace) and 25 cm (photographs of OH radiation). The FRC simulation predicted an onset of ignition at a position of 23 cm while it was artificially set for the zonal EDM at 15.3 cm. Figure 2 (b) compares the different approaches with experimental values of total temperature (T_0) at the combustor exit. The classical EDM

is shown for a constant value $A_{\text{edm}} = 6$ following a parametric study discussed in [23]. The profiles show that the use of the EDM can be greatly improved with an estimate of ignition onset. A very good agreement with experimental values are observed near the wall with the zonal use of the EDM. The FRC (E-S) does perform better than the classic EDM but slightly less than the zonal EDM. This is explained by the fact that the combustion process is kinetically limited until the onset of ignition whereafter it becomes mixing limited. The same observation was made by Kirchhartz et al. [31] in an axisymmetric scramjet combustor with similar fuel injection mechanism. The EDM assumes a mixing limited combustion and is therefore more appropriate once the flow is ignited. Even though the estimated induction length from the one-dimensional program does not agree with experimental observations it proves to be very useful information for an improved use of the EDM. Therefore, the EDM with ignition delay estimate proves to be a viable approach to design scramjet combustors with fuel injection parallel to the air stream.

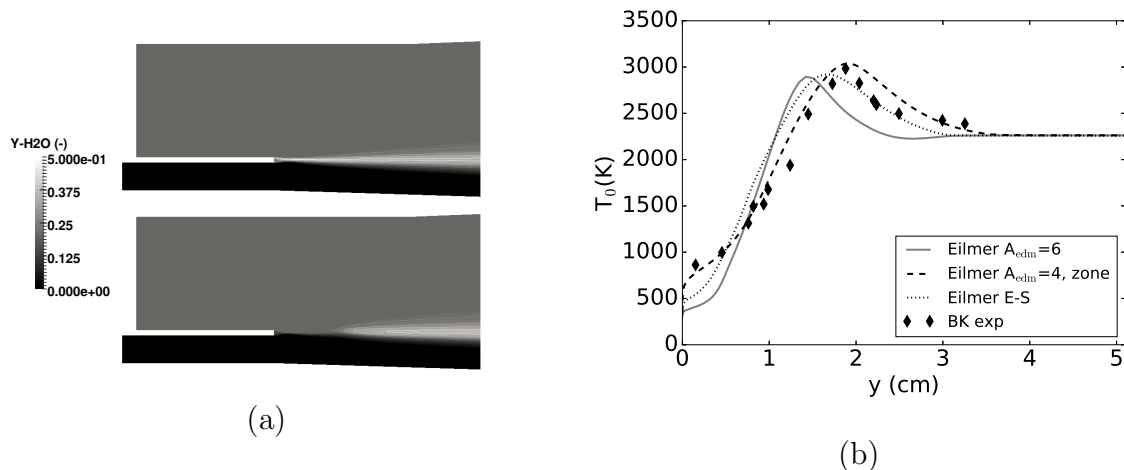


Figure 2: (a) Mass fraction contours of H_2O close to the injection point with top = EDM and bottom = EDM + kinetic limit. (b) total temperature profile at the exit of the combustor ($x = 35.6$ cm).

3.2 HyShot II

The HyShot II combustor was designed for a Mach 8 flight test experiment on supersonic combustion [32, 33]. Experimental campaigns have been undertaken in the HEG Shock tunnel of the DLR with a 1:1 scale representation using hydrogen fuel. The configuration has been studied with different RANS approaches in the literature [32, 33, 34]. A detailed description of the ground test experiment is given by Karl [33] and is considered for numerical study in the present work.

3.2.1 Problem Formulation

Only a part of the combustor, shown in Figure 3, is considered for application of the EDM. It consists of half an injector and two symmetry planes. The injector is modeled as a supersonic inflow boundary with conditions: $w = 1206.7$ m/s , $p = 263720$ Pa, $T = 249$ K, $I = 5$ %, $\mu_t/\mu = 10$. The resulting equivalence ratio is 0.29. The upper and lower boundaries (z coordinates) are treated as viscous isothermal walls at a temperature of 300 K. Compressible wall functions of Nichols and Nelson [35] are adopted as to reduce the computational cost of the simulation due to grid requirements . The computational domain is discretized in 2.784M hexahedral cells and an O-grid topology is adopted for the injector. Inviscid fluxes are treated with the AUSMDV and time stepping with a predictor-corrector scheme. Values for turbulent Prandtl and Schmidt numbers are set to 0.9 and 0.7 respectively. The two-dimensional CFD inflow conditions of Karl et al. [32, 33] are prescribed at the inlet of the three-dimensional domain (same inflow for each lateral cell location) and correspond to averaged conditions: $T = 1300$ K, $p = 130$ kPa, $u = 1720$ m/s and Mach = 2.4. The boundary layer (BL) along the upper wall (cowl side) is assumed to be fully turbulent while a transition from laminar to turbulent flow takes place at the lower wall (injector side) around $x = 45$ mm. This is accounted for in Eilmer by generating two turbulent zones across the width of the domain. Outside these zones the turbulent quantities (k, ω) are purely transported and do not affect the other governing equations.

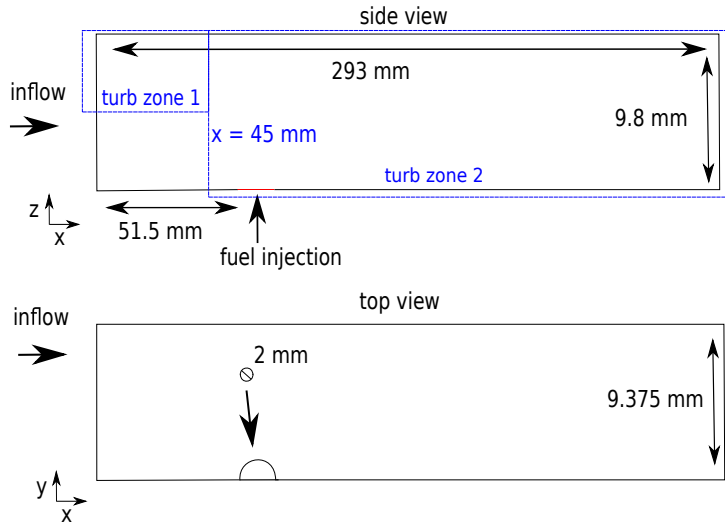


Figure 3: Schematic of the HyShot II combustor [32]. Not to scale.

3.2.2 Results

Figure 4 shows the resulting wall pressure for the injector (a) and cowl (b) side as predicted by Eilmer. The values are taken at the symmetry plane $y = 9.375$ mm. The reacting simulations with the EDM did not converge to a steady-state. This is currently

subject to further investigations. Nevertheless, the unsteady behavior appeared to result in a bounded wall pressure trace indicating that the results are albeit meaningful. Therefore, three curves are represented taken at three distinct times within one flow length (t_1, t_2 and t_3). Also shown, the non-reactive flow field without fuel injection as to give a reference for the pressure rise due to combustion. Moreover, CFD predictions reported in [33] obtained with the Tau code in conjunction with the $k-\omega$ SST model ($Sc_t = 0.35$) and laminar chemistry (modified Jachimowski mechanism) are also plotted. Overall, a good agreement with experimental measurements is observed, especially for the cowl side. On the injector side, near the point of injection (arrow), the EDM profile does not seem to agree well with experiment. The same is true for the Tau reference CFD result. The pressure rise in the recirculation region induced by the injection occurs earlier for the EDM, compared to the laminar chemistry solution. This is most likely due to the strength of the combustion. Karl [33] reports that the flow ignites very close to the point of injection (mixing-limited combustion) with some minor ignition delay. The EDM does not account for that which result in a much higher fuel consumption rate as soon as fuel and oxidizer mix, and therefore a different upstream boundary layer separation zone. Note that Karl [33] does model part of the injector in the simulations which can also contribute to the observed discrepancy. The same comment can be made about the use of wall functions in the present work. Nevertheless, the behavior appears to be localized. The successive complex shock reflection predicted by the EDM differs from the reference solution at the injector side. At the cowl side, similar shock positions are predicted. Karl [33] reports, for a similar setting of Pr_t and Sc_t , that 21 % of the injected hydrogen did not burn by the exit of the combustor. The latter result is obtained with the Spalart-Allmaras turbulence model. In the present work the amount of unburned hydrogen, with $A_{edm}=4$, varies between 35 and 41 %. Note that the exit of the constant area combustor in the present work is 2 cm shorter than the original work. Stream-thrust averages have been computed along the combustor and are given in Figure 5 for variables typically considered in scramjet design with low-fidelity models [36]. The variables are scaled by the reference which is taken as the combustor entrance. Oscillations due to the unsteady character of the CFD solution are visible but variations have a small amplitude and do not affect the global behavior along the combustor. The EDM can therefore replace the low-fidelity approach for the combustor by providing stream-thrust averaged quantities. This study shows that the EDM formulation with standard value for the model constant provides a good agreement with the experiment. The effect of varying this parameter is currently under investigation.

4 CONCLUSIONS

In this work the Eddy Dissipation Model (EDM) has been used in conjunction with Wilcox $k-\omega$ 2006 turbulence model to the study of two scramjet combustors. The designs of both test cases result in high combustor entrance Mach number (> 2) and static temperature (> 1000 K), typical for high flight Mach numbers. In the case of parallel fuel injection, a significant ignition delay is present for which the standard application of the EDM is unable to account. By relying on an estimate of the ignition delay obtained from a

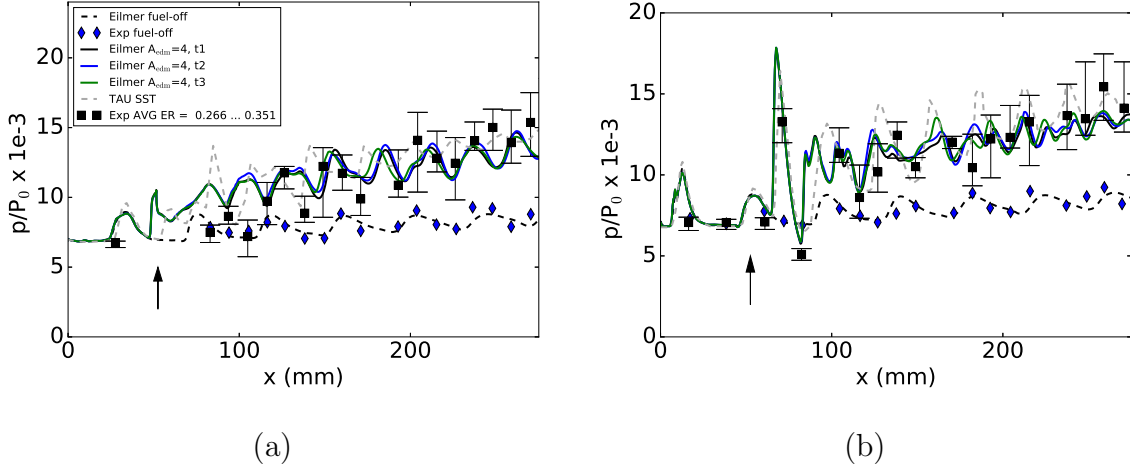


Figure 4: Pressure along the wall at the x - z symmetry plane between the hydrogen injectors. (a) injector side, (b) cowl side. $P_0 = 17.73$ MPa.

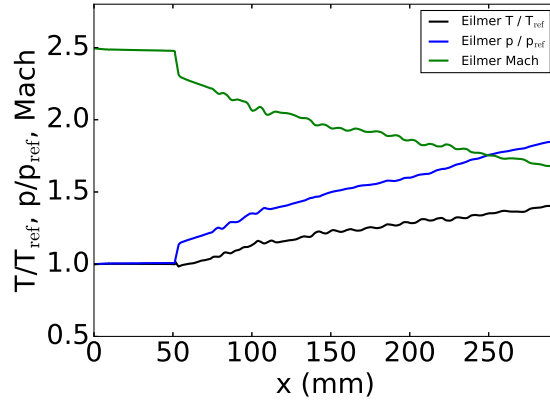


Figure 5: Stream-thrust averaged quantities along the HyShot II combustor. $A_{edm} = 4$, $Pr_t = 0.9$, $Sc_t = 0.7$.

one-dimensional chemical kinetics program, the EDM predictions are in very good agreement with experimental measurements. This indicates that past the point of ignition the combustion appears to be mixing-limited. In the case of transverse fuel injection, ignition occurs almost as soon as the reactants meet, hence mixing-limited combustion is prevalent. The wall pressure traces obtained with the EDM agreed well with experiments for the majority of the combustor length. Some differences are observed at the injector wall, especially near the point of injection. Overall, both studies indicate the potential of the EDM to be considered in the design of scramjet combustors with similar configurations.

Acknowledgements

The first author would like to thank Dr. Sebastian Karl at DLR for providing the inflow conditions of the HyShot II combustor.

REFERENCES

- [1] D Preller and MK Smart. Scramjets for reusable launch of small satellites. In *20th AIAA International Space Planes and Hypersonic Systems and Technologies Conference*, page 3586, 2015.
- [2] SO Forbes-Spyratos, MP Kearney, MK Smart, and IH Jahn. Trajectory design of a rocket-scramjet-rocket multi-stage launch system. In *21st AIAA International Space Planes and Hypersonics Technologies Conference*, page 2107, 2017.
- [3] T.F. O'Brien, R.P. Starkey, and M.J. Lewis. Quasi-one-dimensional high-speed engine model with finite-rate chemistry. *Journal of propulsion and power*, 17(6):1366–1374, 2001.
- [4] T Vanyai, M Bricalli, S Brieschenk, and RR Boyce. Scramjet performance for ideal combustion processes. *Aerospace Science and Technology*, 75:215–226, 2018.
- [5] Sean M Torrez, James F Driscoll, Matthias Ihme, and Matthew L Fotia. Reduced-order modeling of turbulent reacting flows with application to ramjets and scramjets. *Journal of propulsion and power*, 27(2):371–382, 2011.
- [6] RA Baurle. Modeling of high speed reacting flows: established practices and future challenges. *AIAA paper*, 267:2004, 2004.
- [7] NJ Georgiadis, DA Yoder, MA Vyas, and WA Engblom. Status of turbulence modeling for hypersonic propulsion flowpaths. *Theoretical and Computational Fluid Dynamics*, 28(3):295–318, 2014.
- [8] Antonio Ferri. Mixing-controlled supersonic combustion. *Annual Review of Fluid Mechanics*, 5(1):301–338, 1973.
- [9] Antonella Ingenito and Claudio Bruno. Physics and regimes of supersonic combustion. *AIAA Journal*, 48(3):515, 2010.
- [10] Will O Landsberg, Vincent Wheatley, and Ananthanarayanan Veeraragavan. Characteristics of cascaded fuel injectors within an accelerating scramjet combustor. *AIAA Journal*, pages 3692–3700, 2016.
- [11] BF Magnussen and BH Hjertager. On mathematical modeling of turbulent combustion with special emphasis on soot formation and combustion. In *Symposium (international) on Combustion*, volume 16, pages 719–729. Elsevier, 1977.

- [12] JR Edwards and JA Fulton. Development of a RANS and LES/RANS flow solver for high-speed engine flowpath simulations. In *20th AIAA International Space Planes and Hypersonic Systems and Technologies Conference*, page 3570, 2015.
- [13] TO Mohieldin, SN Tiwari, and David E Reubush. Numerical investigation of dual-mode scramjet combustor with large upstream interaction. 2004.
- [14] MSR Chandra Murty and D Chakraborty. Numerical simulation of angular injection of hydrogen fuel in scramjet combustor. *Proceedings of the Institution of Mechanical Engineers, Part G: Journal of Aerospace Engineering*, 226(7):861–872, 2012.
- [15] M Dharavath, P Manna, and D Chakraborty. Thermochemical exploration of hydrogen combustion in generic scramjet combustor. *Aerospace Science and Technology*, 24(1):264–274, 2013.
- [16] O.R. Kummitha, K.M. Pandey, and R. Gupta. Cfd analysis of a scramjet combustor with cavity based flame holders. *Acta Astronautica*, 2018.
- [17] AT Norris. A-priori tuning of modified magnussen combustion model. 2016.
- [18] RJ Gollan and PA Jacobs. About the formulation, verification and validation of the hypersonic flow solver Eilmer. *International Journal for Numerical Methods in Fluids*, 73(1):19–57, 2013.
- [19] PA Jacobs and RJ Gollan. Implementation of a compressible-flow simulation code in the D programming language. In *Applied Mechanics and Materials*, volume 846, pages 54–60. Trans Tech Publ, 2016.
- [20] DC Wilcox. Formulation of the $k-\omega$ turbulence model revisited. *AIAA Journal*, 46(11):2823–2838, 2008.
- [21] WYK Chan, PA Jacobs, and DJ Mee. Suitability of the $k-\omega$ turbulence model for scramjet flowfield simulations. *International Journal for Numerical Methods in Fluids*, 70(4):493–514, 2012.
- [22] JJOE Hoste, V Casseau, M Fossati, IJ Taylor, and RJ Gollan. Numerical modeling and simulation of supersonic flows in propulsion systems by open-source solvers. In *21st AIAA International Space Planes and Hypersonics Technologies Conference, Xiamen, China*, page 2411, 2017.
- [23] JJOE Hoste, M Fossati, IJ Taylor, and RJ Gollan. Modeling scramjet supersonic combustion via eddy dissipation model. In *68th International Astronautical Congress (IAC), Adelaide, Australia*, 2017.
- [24] M.S. Liou. Ten years in the making - AUSM-family. *AIAA Paper*, pages 2001–2521, 2001.

- [25] MN Macrossan. The equilibrium flux method for the calculation of flows with non-equilibrium chemical reactions. *Journal of Computational Physics*, 80(1):204–231, 1989.
- [26] F.R. Menter. Two-equation eddy-viscosity turbulence models for engineering applications. *AIAA Journal*, 32(8):1598–1605, 1994.
- [27] M.C. Burrows and A.P. Kurkov. Analytical and experimental study of supersonic combustion of hydrogen in a vitiated airstream. Technical report, NASA Lewis Research Center, September 1973.
- [28] PG Keistler, RL Gaffney, X Xiao, and HA Hassan. Turbulence modeling for scramjet applications. *AIAA paper*, 5382:2005, 2005.
- [29] WA Engblom, FC Frate, and Nelson CC. Progress in validation of Wind-US for ramjet/scramjet combustion. In *43rd AIAA Aerospace Sciences Meeting and Exhibit*, Reno, Nevada, January 2005.
- [30] V Bhagwandin, W Engblom, and N Georgiadis. Numerical simulation of a hydrogen-fueled dual-mode scramjet engine using Wind-US. In *45th AIAA/ASME/SAE/ASEE Joint Propulsion Conference & Exhibit*, page 5382, 2009.
- [31] RM Kirchhartz, DJ Mee, RJ Stalker, PA Jacobs, and MK Smart. Supersonic boundary-layer combustion: effects of upstream entropy and shear-layer thickness. *Journal of Propulsion and Power*, 26(1):57–66, 2010.
- [32] S. Karl, K. Hannemann, A. Mack, and J. Steelant. CFD analysis of the HyShot II scramjet experiments in the HEG shock tunnel. In *15th AIAA International Space Planes and Hypersonic Systems and Technologies Conference*, page 2548, 2008.
- [33] S Karl. *Numerical investigation of a generic scramjet configuration*. PhD thesis, Saechsische Landesbibliothek-Staats-und Universitaetsbibliothek Dresden, 2011.
- [34] R Pecnik, VE Terrapon, F Ham, G Iaccarino, and H Pitsch. Reynolds-averaged navier-stokes simulations of the hyshot ii scramjet. *AIAA journal*, 50(8):1717–1732, 2012.
- [35] RH Nichols and CC Nelson. Wall function boundary conditions including heat transfer and compressibility. *AIAA journal*, 42(6):1107–1114, 2004.
- [36] MK Smart. How much compression should a scramjet inlet do? *AIAA journal*, 50(3):610–619, 2012.